



Bone regeneration: The influence of composite HA/TCP scaffolds and electrical stimulation on TGF/BMP and RANK/RANKL/OPG pathways

Júlia Venturini Helaehil^{a,b} , Boyang Huang^c , Paulo Bartolo^c , Milton Santamaria-JR^{a,d,e} ,
Guilherme Ferreira Caetano^{a,b,d,*} 

^a University Center of Hermínio Ometto Foundation, FHO, Araras 13607-339, SP, Brazil

^b Division of Dermatology, Department of Internal Medicine, Ribeirão Preto Medical School, University of São Paulo, São Paulo 05508-060, Brazil

^c Singapore Centre for 3D Printing, School of Mechanical and Aerospace Engineering, Nanyang Technological University, Singapore 639798, Singapore

^d Graduate Program of Orthodontics, University Center of Hermínio Ometto Foundation, FHO, Araras 13607-339, SP, Brazil

^e Department of Social and Pediatric Dentistry, Institute of Science and Technology, São Paulo State University - Unesp, São José dos Campos, 12245-000, Brazil

ARTICLE INFO

Keywords:

Bioprinting
Electrical stimulation
Microcurrent
TGF pathway
Tissue engineering

ABSTRACT

The repair of critical-sized bone defects represents significant clinical challenge. An alternative approach is the use of 3D composite scaffolds to support bone regeneration. Hydroxyapatite (HA) and tri-calcium phosphate (β -TCP), combined with polycaprolactone (PCL), offer promising mechanical resistance and biocompatibility. Bioelectrical stimulation (ES) at physiological levels is proposed to reestablishes tissue bioelectricity and modulates cell signaling communication, such as the BMP/TGF- β and the RANK/RANK-L/OPG pathways. This study aimed to evaluate the use HA/TCP scaffolds and ES therapy for bone regeneration and their impact on the TGF- β /BMP pathway, alongside their relationship with the RANK/RANKL/OPG pathway in critical bone defects. The scaffolds were implanted at the bone defect in animal model (calvarial bone) and the area was subjected to ES application twice a week at 10 μ A intensity of current for 5 min each session. Samples were collected for histomorphometry, immunohistochemistry, and molecular analysis. The TGF- β /BMP pathway study showed the HA/TCP+ES group increased BMP-7 gene expression at 30 and 60 days, and also greater endothelial vascular formation. Moreover, the HA/TCP and HA/TCP+ES groups exhibited a bone remodeling profile, indicated by RANKL/OPG ratio. HA/TCP scaffolds with ES enhanced vascular formation and mineralization initially, while modulation of the BMP/TGF pathway maintained bone homeostasis, controlling resorption via ES with HA/TCP.

Introduction

Bone tissue is a type of connective tissue that provides support, protection, and helps maintain homeostasis [1]. In addition to high dynamism, this tissue presents piezoelectric effects which are important for promoting the repair and healing process [2]. Although this tissue has self-healing capacity, critical defects lead to a considerable loss of electrical potential at the injured site, requiring the use of grafts or additional therapies [1,2]

Autogenous grafts are considered the most effective option for bone regeneration due to their osteoinductive, osteoconductive and osteogenic properties, which means these contain living bone cells, including osteoblasts, which have the ability to directly form new bone, and also are able to stimulate the surrounding undifferentiated mesenchymal stem cells (MSCs) to differentiate into osteoblasts, leading to new bone

formation and act as scaffolds. However, there are clinical limitations associated with their use, such as the need for secondary surgeries and anatomical constraints [3–5].

Another approach is the use of allografts. Allografts are bone grafts sourced from a donor of the same species and are primarily osteoconductive, providing a scaffold for bone growth, with limited osteoinductive properties and no osteogenic potential. They offer convenience due to availability, but there are several complications including the risk of immune rejection, disease transmission, graft resorption, and failure or non-union. Despite these risks, allografts are widely used in clinical settings as an alternative to autografts, especially when a secondary surgical site is not desirable [1,5–7].

To overcome these challenges, various bone substitutes have been developed through advancements in bone tissue engineering (BTE). One of the most promising is the use of 3D scaffolds produced in a laboratory.

* Corresponding author.

E-mail address: caetanogf@fho.edu.br (G.F. Caetano).

<https://doi.org/10.1016/j.injury.2025.112158>

Accepted 6 January 2025

Available online 12 January 2025

0020-1383/© 2025 Elsevier Ltd. All rights are reserved, including those for text and data mining, AI training, and similar technologies.

The literature has highlighted that the composition and structure of scaffolds are crucial for their success. When designing scaffolds, it is important to consider the material's ability to interact with the extracellular matrix (ECM) and promote cell differentiation and proliferation. The material must also be biocompatible, biodegradable, and able to induce osteogenesis and angiogenesis i.e. osteoinduction and osteoconduction [1,4,5].

The materials commonly used for BTE application are bioglass, metals, polymers, ceramics, and calcium phosphate ceramics, particularly hydroxyapatite. ($\text{Ca}_{10}(\text{PO}_4)_6(\text{OH})_2$; HA) and tri-calcium phosphate ($\beta\text{-Ca}_3(\text{PO}_4)_2$; β -TCP) has shown promising results in the literature due to its biocompatibility and chemical similarity with natural bone tissue's inorganic components [3,5–7]. Scaffolds made of HA/TCP only have certain disadvantages such as low mechanical resistance and high brittleness at high concentrations. However, by combining ceramic materials with aliphatic polymers like polycaprolactone (PCL), these issues can be overcome due to the adequate mechanical resistance and biocompatibility of the polymer. This results in a scaffold with superior mechanical and osteogenic properties [3,5–7].

To recover the significant loss of hydroxyapatite (HA) in critical bone defects and aid in restoring the lost electrical potential, combining non-invasive exogenous therapies, such as low-intensity electrical stimulation (ES), is proposed. This approach can facilitate the organization of collagen fibers during the repair process, promoting both tissue repair and the restoration of its electrical potential [3,8].

The ES is a commonly used technique to stimulate cells due to its non-invasive nature and ease of application. At physiological levels, it has been demonstrated to stimulate cell migration, proliferation, and differentiation in bone tissue, resulting in enhanced bone formation and mineralization. Additionally, this stimulation promotes the synthesis of cytokines and growth factors, such as VEGF and BMP-7 [7–10].

The Bone morphogenetic protein-7 (BMP-7) is an important member of the transforming growth factor β (TGF- β) superfamily, where it induces the expression of osteoblast differentiation markers and promotes angiogenesis. Generally, the BMP and TGF- β signaling pathway play crucial roles in the development and maintenance of bone homeostasis. TGF- β 1 is a protein that promotes the proliferation and differentiation of osteoblasts and inhibits osteoclast formation, reducing RANKL expression while increasing OPG expression [10–12].

However, the literature still does not report the effects of the association between HA/TCP scaffolds and electrical stimulation and their effects on signaling pathways, such as the TGF- β /BMP pathway and their relationship with the RANK/RANKL/OPG pathway. Therefore, the aim of this study was to evaluate the use of composite scaffolds of polycaprolactone (PCL) associated with hydroxyapatite and tricalcium phosphate (HA/TCP) subjected to electrical stimulation in bone regeneration and its effects on the TGF- β /BMP pathway and its relationship with the RANK/RANKL/OPG pathway in critical bone defects.

Materials and methods

Scaffold fabrication

PCL pellets (Perstorp Caprolactones, Cheshire, UK) were heated to 90 °C and mixed for 20 min with 10 % wt of HA nanoparticles (Sigma-Aldrich, St. Louis, USA) and 10 % wt of TCP microparticles (Sigma-Aldrich, St. Louis, USA), resulting in a mixture comprising 80 % PCL + 10 % wt HA + 10 % wt TCP. The composite material was then 3D printed using a screw-assisted 3D Discovery printer (REGENHU, Villaz-Saint-Pierre, Switzerland), employing a 0/90° lay-down pattern. Subsequently, the fabricated scaffolds were sterilized in 70 % ethanol for 4 h and rinsed with a sterile solution.

The scaffolds used in the animal experiments (bone graft) were composed of polycaprolactone (PCL) and a mixture of polycaprolactone with 10 % hydroxyapatite and 10 % tricalcium phosphate (HA/TCP). They were precisely cut to match the size of the bone defects created in

the animals (5mm x 5 mm), grafted on the day of surgery, and remained implanted in the animals for experimental periods of 30 and 60 days.

In vivo study

All surgical and experimental procedures were conducted in accordance with established experimental standards and biodiversity regulations (NIH Publication 80–23, revised 1996, and Arouca Law-11,794, 2008). These procedures were approved by the Ethics Committee on Animal Use of the Hermínio Ometto Foundation, following ethical principles in animal research (CEUA 075/2017). The rats were randomly allocated into four experimental groups, as detailed in Table 1, and were investigated through two experimental periods: 30 and 60 days.

The animals were randomly assigned to one of four experimental groups: PCL (bone defect was treated with PCL scaffolds), PCL+ES (bone defect was treated with PCL scaffolds and also the application of electrical stimulation), HA/TCP (bone defect was treated with composite scaffolds of 80 % PCL + 10 % hydroxyapatite + 10 % tricalcium phosphate), and HA/TCP+ES (bone defect was treated with composite scaffolds of 80 % PCL + 10 % hydroxyapatite + 10 % tricalcium phosphate and also the application of electrical stimulation).

Surgical protocol

The animals underwent anesthesia through intraperitoneal administration of a mixture containing ketamine hydrochloride (30 mg/kg) and xylazine hydrochloride (10 mg/kg). Following this, the occipital region of the animals was shaved. A critical-sized bone defect measuring 5 mm × 5 mm was then created at the center of the calvarial bone, with continuous irrigation using physiological solution (NaCl 0.9 %). This procedure was performed using an Osteo I tip (Piezo Helse, Helse Dental Technology, Santa Rosa do Viterbo, SP, Brazil) attached to a dental ultrasound handpiece (Olsen, Palhoça, SC, Brazil).

The scaffolds underwent sterilization in 70 % ethanol prior to precise fitting into the bone defect, eliminating the need for clamping or physical fixation. Following scaffold implantation, the wounds were closed with nylon 5–0 sutures (Shalon Medical, Goiânia, Brazil), and the animals received intraperitoneal and oral analgesic treatments consisting of tramadol hydrochloride (1 mg/kg) and dipyrone (50 mg/kg), respectively, for 72 h. Throughout this period, the animals were closely monitored by the researchers.

Electrical stimulation and post treatment

Exogenous electrical stimulation (ES) was conducted using a low-intensity transcutaneous electrical stimulator (Physectonus micro-current, BIOSET, Indústria de Tecnologia Eletrônica Ltda, Rio Claro, São Paulo, Brazil). Two conductive metal electrodes with 10 mm diameter probes were gently placed in contact with the animal's head, encircling the bone defect, for 5 min at 10 μ A (galvanic electrical current), twice a week, throughout the experimental periods. The ES protocol and its potential on bone regeneration have been previously reported by Helaehil et al. [7].

Samples were collected, encompassing the entire area of the bone

Table 1
Experimental groups for *in vivo* study.

Group name	Electrical Stimulation	PCL Polymer Concentration	Ceramic Concentration
PCL	No	100 wt%	0 wt%
PCL+ES	Yes	100 wt%	0 wt%
HA/TCP	No	80 wt%	HA 10 wt% + TCP 10 wt%
HA/TCP+ES	Yes	80 wt%	HA 10 wt% + TCP 10 wt%

defect/scaffold (representing new tissue formation) and approximately 2 mm of the bone edges. From each group, three samples were obtained for histomorphometric and immunohistochemical analysis ($n = 3/\text{group/experimental period}$), immediately fixed in 10 % formaldehyde for 48 h. Additionally, five samples from each group were promptly frozen at $-80\text{ }^{\circ}\text{C}$ in 2 mL plastic tubes for molecular evaluation ($n = 5/\text{group/experimental period}$).

Histomorphometry

After 48 h of fixation, the samples were transferred to a 50 % buffered formic acid decalcifying solution (Morse’s decalcifying) for a period of 45 days, with the solution being changed three times per week. Following demineralization, the samples underwent a 1 h wash in running water, followed by dehydration in increasing concentrations of ethanol, diaphanization with xylene, and embedding in paraffin. Subsequently, the samples were sectioned into $4.0\text{ }\mu\text{m}$ thick slices and mounted on glass slides. Masson’s Trichrome (MT) staining was performed for histomorphometric evaluation.

Histological images were captured using a Leica DM2000 microscope (Leica Microsystems, Wetzlar, Germany). The MT-stained samples were captured at $200\times$ magnification for histomorphometric analysis, including the assessment of the number of blood vessels, vascular area, osteoid/collagen tissue, and mineralized tissue. Ten images from each bone sample (each animal) were analyzed using *ImageJ* software.

Immunohistochemistry

The histological samples, with cross-sections measuring $4.0\text{ }\mu\text{m}$, were mounted on silanized slides and subjected to incubation with specific primary antibodies (as listed in Table 2) to assess bone formation and remodeling processes. Subsequently, secondary antibodies and the antibody detection reaction (utilizing Novolink™ Max Polymer Detection System) were applied according to the manufacturer’s recommended protocol (Leica Biosystems, Buffalo Grove, IL, USA). Diaminobenzidine (DAB) served as the substrate chromogen to visualize the specific markings, followed by counterstaining with Harris hematoxylin.

Eight images from each bone sample were captured at $400\times$ magnification using a Leica DM2000 microscope (Leica Microsystems, Wetzlar, Germany), and the quantification was conducted using *ImageJ* software.

Quantitative polymerase chain reaction (RT-qPCR)

The samples were collected at 30 and 60 days post-surgery and subsequently macerated using liquid nitrogen. Total RNA was isolated using TRIzol™ reagent (Invitrogen, Waltham, MA, USA), following the manufacturer’s instructions. Cell lysis was achieved using a homogenizer (Polytron System PT 1200E, Kinematica AG, Malters, Switzerland). The quality and quantity of RNA samples were assessed using a spectrophotometer to determine the A260/230 and A260/280 ratios. cDNA was synthesized from $1.5\text{ }\mu\text{g}$ of total RNA using the high-capacity kit (Thermo Fisher Scientific, code 4,374,966) according to the manufacturer’s instructions. Gene expression analyses were performed in triplicate using 5 ng of cDNA, 300 nM of each primer, and $1\times$ of Master Mix. For SYBR Green PCR Master Mix, the amplification was carried out in QuantStudio3™ (Applied Biosystems) with the following parameters:

Table 2
Antibodies used for immunostaining.

Antibody	Dilution	Codes	Company
RANK-L	1:200	sc-377,079	Santa Cruz Biotechnology, USA
OPG	1:200	sc-390,518	
TGF- β	1:250	sc-130,348	
BMP-7	1:500	FNAB00920	Fine Test

initial denaturation at $50\text{ }^{\circ}\text{C}$ for 2 min, followed by $95\text{ }^{\circ}\text{C}$ for 2 min, then 40 cycles of denaturation at $95\text{ }^{\circ}\text{C}$ for 15 s, and annealing/extension at $60\text{ }^{\circ}\text{C}$ for 1 min. For TaqMan Gene Expression Master Mix, the thermal cycling conditions were $95\text{ }^{\circ}\text{C}$ for 10 min, followed by 45 cycles at $95\text{ }^{\circ}\text{C}$ for 15 s and $60\text{ }^{\circ}\text{C}$ for 1 min. Expression levels were normalized to *Actb* for SYBR Green and *Gapdh* for TaqMan and validated using the *Best-Keeper* software, which was also used as the normalizer. The PCL group served as the calibrator. Results were calculated using the $2^{-\Delta\Delta\text{Ct}}$ method. Primer sequences are provided in Table 3, and the probes in Table 4.

Statistical analysis

All experimental data are presented as the mean \pm standard error of the mean. Data were analyzed using *GraphPad Prism 8* software (GraphPad Software, San Diego, CA, USA) and verified using the Shapiro-Wilk normality test. One-way ANOVA with Tukey’s post-hoc test was applied for parametric data, while the Kruskal–Wallis test with Dunn post-hoc, was applied for non-parametric data. Significance levels were set at: * $p < 0.05$; ** $p < 0.01$; *** $p < 0.001$; **** $p < 0.005$.

Results

BMP/TGF signalling pathway

Fig. 1 demonstrates the relative expression of the *Bmp-7* and *Tgf- β* genes at 30 and 60 days. Fig. 1a shows that the both HA/TCP groups presented three times the fold change of PCL group, however no statistical evidence was observed at 30 days. Moreover, HA/TCP+ES group showed lower *Bmp-7* expression compared to the PCL group at 60 days. In Fig. 1b), the HA/TCP group exhibited forty times the fold change of *Tgf- β* when compared to the HA/TCP+ES group at 60 days.

The percentage of positive area for BMP-7 and the number of positive cells for TGF- β at 30 and 60 days are shown in Fig. 2. There was no significant difference in BMP-7 between the groups at either the 30-day or 60-day mark. However, at 30 days, the HA/TCP group exhibited a higher quantity of marked TGF- β cells compared to the PCL group. By 60 days, the HA/TCP group showed a greater number of positive cells than the HA/TCP+ES group.

Bone formation

Angiogenesis

Fig. 3 presents the number of blood vessels and vascular area at 30 and 60 days. There were no significant differences in the number of vessels among the groups at 30 and 60 days. No statistical difference was observed for vascular area evaluation. However, it was observed an increasing in HA/TCP group at 30 days.

Mineralization

The osteoid tissue and mineralized tissue area at 30 and 60 days is shown in Fig. 4. At 30 days, the HA/TCP group exhibited higher percentage of osteoid area compared to the PCL group, but lower percentage compared to the PCL+ES group at 60 days. No differences were observed among the groups at 30 days for mineralized tissue area. However, the PCL+ES and HA/TCP groups displayed smaller mineralized area compared to the PCL and HA/TCP+ES groups. At 60 days, the

Table 3
SYBER Green primers used in the RT-qPCR.

Gene	Forward (5’ – 3’)	Reverse (5’ – 3’)
Rank	CGTCTGCTCCTTTCATCTCT	CCCTGAGGACTCCTTATTTCGA
<i>Rank-1</i>	AGCGCAGATGGATCCTAACAA	TCGAGTCTTGCAAACCTGTA
<i>Opg</i>	GAGTGTGCGAATGTGAGGAA	TGCTTTCGATGACGTCTCAC
<i>Actb1</i>	AGAGGGAAATCGTGCGTGACA	CGATAGTGATGACCTGACCGTCA

Table 4
TaqMan Assays used in the RT-qPCR.

TaqMan Assays	Product codes
<i>Gapdh</i> Glyceraldehyde-3-Phosphate Dehydrogenase	Rn01775763_g1
<i>Bmp-7</i> Bone morphogenetic protein-7	Rn01528889_m1
<i>Tgf-β</i> Transforming growth factor β	Rn00572010_m1

HA/TCP group demonstrated greater mineralized area compared to the PCL+ES group, and higher than the others.

Bone remodelling

Fig. 5 shows the relative expression of *Rank*, *Rankl*, *Opg*, and *Rankl/Opg* ratio at 30 and 60 days. The gene expression of *Rank*, *Opg*, and *Rankl/Opg* ratio did not show differences among the groups at 30 and 60 days. At 30 days, the PCL+ES group exhibited higher expression of *Rankl*

compared to PCL, HA/TCP, and HA/TCP+ES. However, no differences were observed among the groups at 60 days. *Rankl/Opg* ratio demonstrates the HA/TCP group at 30 days presented unbalanced.

Fig. 6 presents the quantification of RANKL-positive cells, OPG-positive cells, and the RANKL/OPG ratio at 30 and 60 days. After 30 days, the PCL group showed a greater positive cells compared to the HA/TCP and HA/TCP+ES groups regarding RANK-L marking. During the same period, the PCL and PCL+ES groups showed a greater number of cells than the HA/TCP and HA/TCP+ES groups at 30 days. However, by 60 days, all four groups demonstrated similar cell counts.

The graph depicting the RANKL/OPG ratio reveals that the PCL, HA/TCP, and HA/TCP+ES groups exhibited values greater than 1 at 30 days, indicative of a tendency towards bone resorption. Conversely, the PCL+ES group presented a ratio lower than 1 at 30 days. At 60 days, a similar pattern persisted, with the PCL and PCL+ES groups showing values close to 1, while the HA/TCP and HA/TCP+ES groups continued to display values above 1, indicating a continued tendency towards bone resorption.

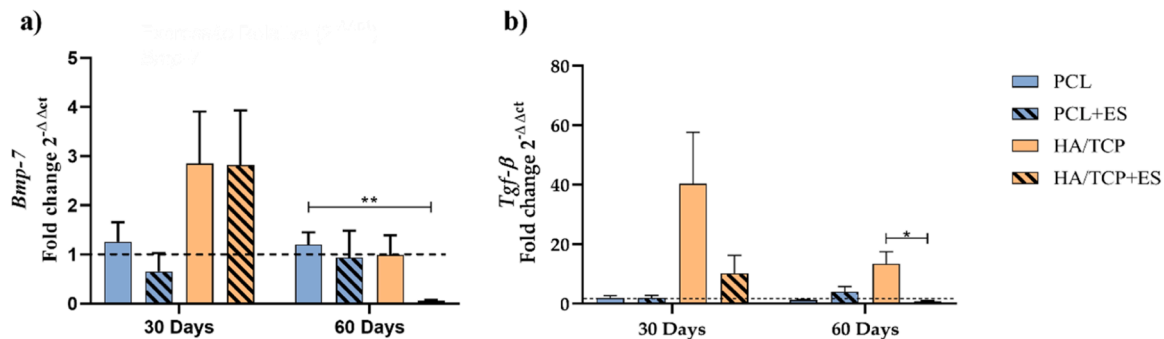


Fig. 1. Relative expression of (a) *Bmp-7* and (b) *Tgf-β* at 30 and 60 days. Results were expressed as mean ± standard error of the mean (significance levels were established in * $p < 0.05$, ** $p < 0.01$).

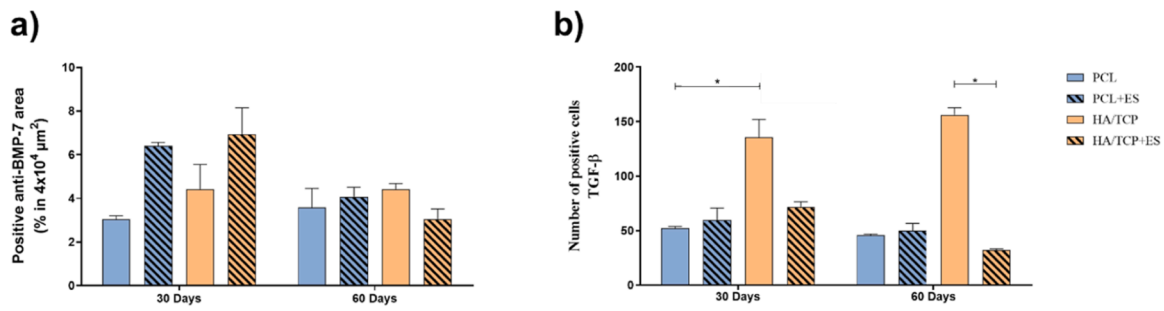


Fig. 2. Evaluation of immunomarking of (a) positive area anti-BMP-7 and (b) number of positive cells anti-TGF-β at 30 and 60 days. Results were expressed as mean ± standard error of the mean (significance levels were established in * $p < 0.05$, ** $p < 0.01$, *** $p < 0.001$, **** $p < 0.0005$).

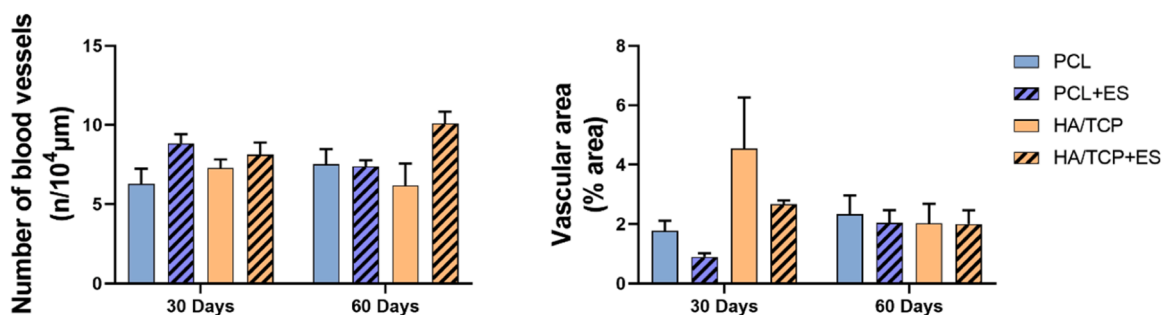


Fig. 3. Evaluation of angiogenesis by (a) number of blood vessels and (b) vascular area at 30 and 60 days. Results were expressed as mean ± standard error of the mean (significance levels were established in * $p < 0.05$).

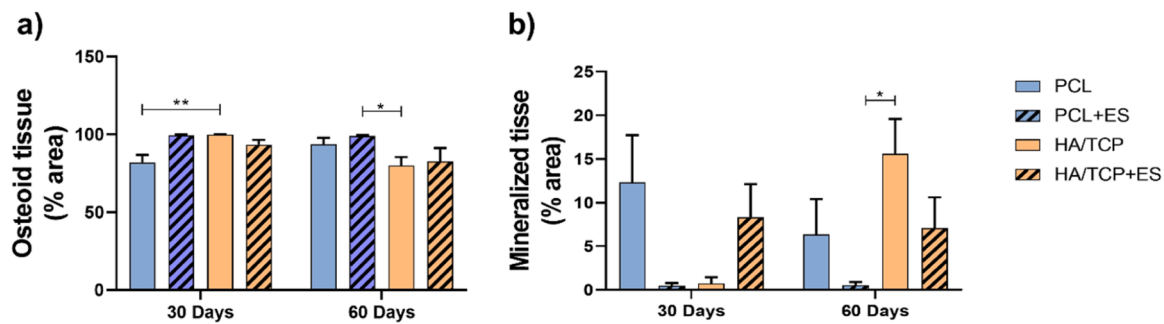


Fig. 4. Evaluation of mineralization by (a) percentage of osteoid tissue and (b) percentage of mineralized tissue after 30 and 60 days. Images stained with Masson's trichrome at 200x magnification were used for quantification. Results were expressed as mean \pm standard error of the mean (significance levels were established in * $p < 0.05$, ** $p < 0.01$).

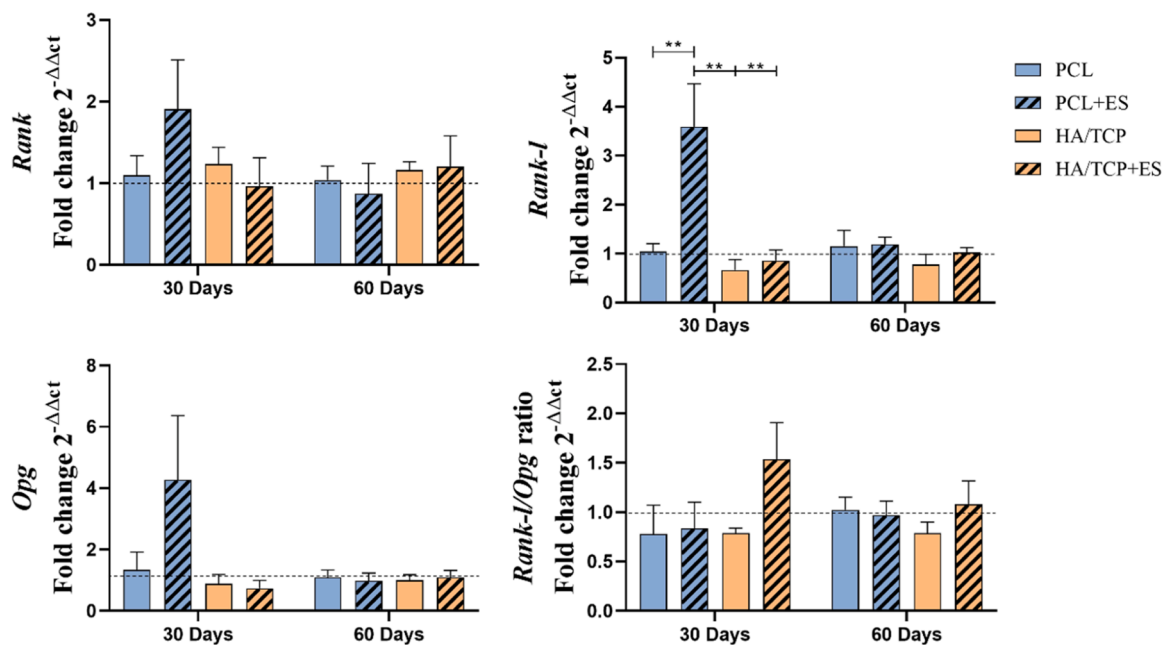


Fig. 5. Relative expression of (a) *Rank*, (b) *Rank-1*, (c) *Opg* and (d) *Rank-1/Opg* $2^{-\Delta\Delta Ct}$ at 30 and 60 days. Results were expressed as mean \pm standard error of the mean (significance levels were established in ** $p < 0.01$).

Discussion

The TGF- β and BMP signaling pathways regulate a variety of physiological and pathological processes, especially in bone tissue. The activation of TGF- β is believed to be regulated mechanically in the superficial region of the lesion rather than through the application of electrical stimuli. During tissue regeneration, mechanical activation is expected to change as tissue maturation occurs, along with the deposition of an extracellular matrix that will bind to TGF- β [13,14]. BMPs (bone morphogenic proteins) are part of the transforming growth factor-beta superfamily. Their actions are regulated by receptor kinases and transcription factors called Smads. Among these proteins, BMP-2, 4, 6, 7, and 9 are identified as inducers of bone growth [15].

The elevated expression of *Bmp-7* at 30 days by the HA/TCP and HA/TCP+ES groups may be an important event to support osteogenesis, especially during the early stages of bone formation, in association with along with *Bmp-2*, *Bmp-4*, and GDF5, for example [11,12]. After tissue mineralization, there is a decrease in the expression levels of *Bmps*, consistent with the results obtained from the HA/TCP groups and, especially, the HA/TCP+ES group regarding the expression of *Bmp-7*, along with the greater formation of mineralized tissue presented in both groups at the 60 days.

Angiogenesis is a crucial event for bone formation. Several studies have demonstrated the angiogenic and osteogenic effects of ES in bone tissue, especially when associated with ceramic scaffolds [3,7,8,11]. ES application can promote important angiogenic responses of vascular endothelial cells and regulate the production of growth factors like VEGF and BMP-7 [8]. Our results demonstrated the use of scaffolds associated with electrical stimulation (HA/TCP+ES group), presented greater stimulus to vascularization, which could explain the enhanced BMP/TGF signalling. Moreover, although TGF- β and BMP-7 are directly related to the angiogenesis process, both can also contribute to the process of mineralization.

Several hypotheses have been developed to elucidate the therapeutic or biological effects of electric fields on bone tissue [2,16,17]. Electrical stimulation can aid in bone formation and the optimal intensities for bone formation and mineralization range between 1 and 20 uA [18].

Mineralization can be considered the final hallmark of the osteoblastic differentiation process [19]. The association of HA/ β -TCP promoted osteoinductive and osteoconductive conditions to the scaffold, favoring bone formation [3,20]. This can be confirmed by the results obtained regarding the osteoid tissue area, where all groups exhibited tissue formation, along with the higher quantity of mineralized tissue area observed in the HA/TCP+ES group at both 30 and 120 days.

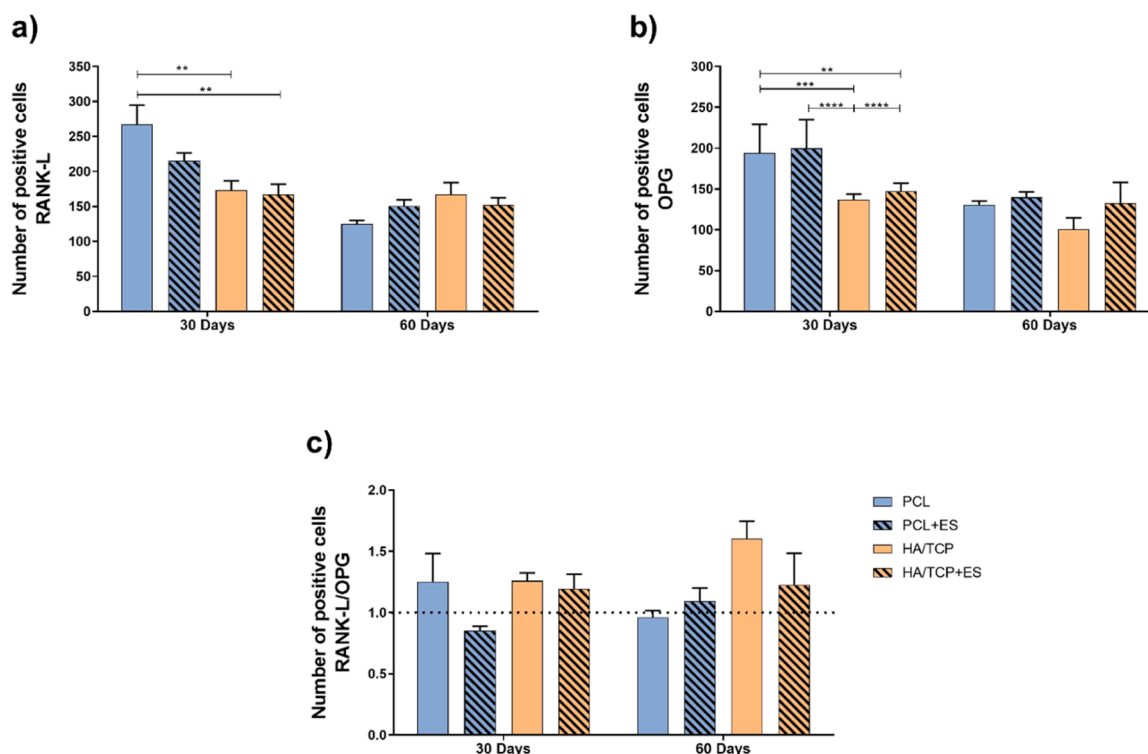


Fig. 6. Evaluation of immunomarking of (a) number of positive cells anti-RANK-L, (b) number of positive cells anti-OPG and (c) RANK-L/OPG ratio 30 and 60 days. Results were expressed as mean \pm standard error of the mean (significance levels were established in ** $p < 0.01$, *** $p < 0.001$, **** $p < 0.005$).

Leppik et al. [8] report that after the application of ES in the *in vivo* assay, there was a significant increase in TGF- β expression in the eighth week of treatment. However, our results demonstrate that the HA/TCP group showed higher expression compared to the group that received ES application, which was confirmed by TGF- β positive cells observed on the tissue for both 30 and 60 experimental days. The enhanced mineralization observed in the HA/TCP+ES group at 30 days, it is plausible that the peak expression of TGF- β occurred during periods preceding the 30th day. Furthermore, Leppik et al. [21] reported in another study that the expression of TGF- β was elevated at 3, 7, and 14 days when stem cells were cultured on β -TCP scaffolds along with ES application. However, at 21 days, there was a decrease in TGF- β expression, an event that is consistent with the results observed at the 30 days. These findings suggest that the ES protocol used is advisable for application at the early stages of bone regeneration involving grafts (scaffolds), as it rapidly stimulated factors associated with osteogenesis, including the TGF- β pathway evaluated in this research work, enhancing mineralization.

In turn, TGF- β plays a crucial role in connective tissue regeneration and bone remodeling with significant effects on osteogenic differentiation and bone formation [22]. Some studies suggest that using β -TCP can increase bone formation and the expression of BMPs along with TGF- β [21]. The literature suggests that while the combination of HA/TCP is effective due to its osteoconductive and osteoinductive characteristics. The expression of TGF- β was found to be similar in scaffolds with different concentrations of HA/TCP when compared to scaffolds composed only of β -TCP [23]. Another point to consider is that β -TCP scaffolds exhibited a positive response to electrical stimulation [17], while the combination of both compounds did not.

TGF- β is also responsible for inhibiting bone formation in the late stages of osteoblastic differentiation, directly influencing the RANKL/OPG pathway [11,12,24]. Therefore, low gene expression and TGF- β positive cells may be directly related to maintaining the balance of bone homeostasis when the resorption (bone remodeling) process is predominant. This event justifies the results obtained regarding the expression of TGF- β at 30 and 60 days in the HA/TCP+ES group, along

with the OPG, once these may be modified according to the electrical stimulus [19,24]. It is also possible to observe a direct relationship with values above 1 regarding the RANKL/OPG ratio, where values above 1 indicated a tendency toward the bone resorption process in the same experimental periods. Another notable observation was the higher mineralization in the HA/TCP+ES group at day 30, which was lower than that of the HA/TCP group by day 60. This outcome could be linked to the higher RANKL/OPG gene expression ratio observed at day 30, suggesting a more pronounced resorption phase occurring between days 30 and 60. The reduced mineralization at day 60 may indicate that the newly formed bone had entered the remodeling phase, reflecting a progression toward more advanced bone regeneration.

In normal conditions RANK/RANKL interaction is regulated by the OPG decoy receptor that by blocking RANKL promotes bone formation [25]. The increase in relative expression of *Bmp-7* at 30 days by the HA/TCP and HA/TCP+ES groups is also related to the osteoclastic formation process, as *Bmp-7* stimulates the formation of osteoclasts by increasing the expression levels of *Rank* [12]. This event was observed in the relative expression results at the 30 days in the HA/TCP and HA/TCP+ES groups.

It's important to note that previous studies have shown the impact of using electrical stimulation (ES) on scaffolds made of HA/TCP on other pathways, such as the Wnt/Beta-catenin pathway and the Ca²⁺/CaM pathway. It was previously observed that both pathways exhibited a higher rate of mineralization compared to groups that did not receive ES [3]. Therefore, each signaling pathway may respond differently to electrical stimuli.

Conclusion

It can be concluded that the combination of polymeric/ceramic (composite) scaffolds of HA/TCP associated with ES could be used for bone regeneration, preferably at the early stages of bone repair treatment in terms of BMP/TGF pathway. HA/TCP scaffolds without ES showed a better response in terms of modulating the BMP/TGF pathway

in both experimental periods. Finally, HA/TCP scaffolds with and without ES application showed greater mineralization and were able to modulate the BMP/TGF pathway for the maintenance of bone homeostasis associated with the RANK/RANKL/OPG triad, controlling the bone resorption process through the application of ES associated with the HA/TCP scaffold graft. By using composite scaffolds produced with PCL, HA and TCP, the authors believe the ES application is important at the early stages of bone regeneration to modulate and stimulate bone formation pathways, once the endogenous bioelectricity is impaired.

Funding

This project was partially supported by the São Paulo Research Foundation (FAPESP), grants numbers 2018/21167-4 and 2016/23237-4 and also by CNPq (“Conselho Nacional do desenvolvimento Científico e Tecnológico”) grant number 423710/2018-4.

CRediT authorship contribution statement

Júlia Venturini Helaehil: Writing – review & editing, Writing – original draft, Methodology, Investigation, Formal analysis, Data curation. **Boyang Huang:** Writing – review & editing, Visualization, Software. **Paulo Bartolo:** Writing – review & editing, Validation, Investigation, Funding acquisition, Conceptualization. **Milton Santamaria-JR:** Writing – review & editing, Validation, Supervision, Project administration, Investigation, Formal analysis, Conceptualization. **Guilherme Ferreira Caetano:** Writing – review & editing, Visualization, Validation, Supervision, Resources, Project administration, Investigation, Funding acquisition, Conceptualization.

Declaration of competing interest

None.

References

- [1] Koushik TM, Miller CM, Antunes E. Bone tissue engineering scaffolds: function of multi-material hierarchically structured scaffolds. *Adv Healthc Mater* 2023;12. <https://doi.org/10.1002/adhm.202202766>.
- [2] Oladapo BI, Ismail SO, Kayode JF, Ikumapayi OM. Piezoelectric effects on bone modeling for enhanced sustainability. *Mater Chem Phys* 2023;305. <https://doi.org/10.1016/j.matchemphys.2023.127960>.
- [3] Helaehil JV, Helaehil LV, Alves LF, Huang B, Santamaria-Jr M, Bartolo P, Caetano GF. Electrical stimulation therapy and HA/TCP composite scaffolds modulate the wnt pathways in bone regeneration of critical-sized defects. *Bioengineering* 2023;10:75. <https://doi.org/10.3390/bioengineering10010075>.
- [4] Rodríguez-Merchán EC. Bone healing materials in the treatment of recalcitrant nonunions and bone defects. *Int J Mol Sci* 2022;23:3352. <https://doi.org/10.3390/ijms23063352>.
- [5] Roseti L, Parisi V, Petretta M, Cavallo C, Desando G, Bartolotti I, Grigolo B. Scaffolds for bone tissue engineering: state of the art and new perspectives. *Mater Sci Eng* 2017;78:1246–62. <https://doi.org/10.1016/j.msec.2017.05.017>.
- [6] Bohner M, Santoni BLG, Döbelin N. β -tricalcium phosphate for bone substitution: synthesis and properties. *Acta Biomater* 2020;113:23–41. <https://doi.org/10.1016/j.actbio.2020.06.022>.
- [7] Helaehil JV, Lourenço CB, Huang B, Helaehil LV, de Camargo IX, Chiarotto GB, Santamaria-Jr M, Bártolo P, Caetano GF. *In vivo* investigation of polymer-ceramic PCL/HA and PCL/ β -TCP 3D composite scaffolds and electrical stimulation for bone regeneration. *Polymers (Basel)* 2021;14:65. <https://doi.org/10.3390/polym14010065>.
- [8] Leppik L, Oliveira KMC, Bhavsar MB, Barker JH. Electrical stimulation in bone tissue engineering treatments. *Euro J Trauma Emerg Surg* 2020;46:231–44. <https://doi.org/10.1007/s00068-020-01324-1>.
- [9] Pettersen E, Anderson J, Ortiz-Catalan M. Electrical stimulation to promote osseointegration of bone anchoring implants: a topical review. *J Neuroeng Rehabil* 2022;19:31. <https://doi.org/10.1186/s12984-022-01005-7>.
- [10] Wang Z, Hutton WC, Yoon ST. The effect of capacitively coupled (CC) electrical stimulation on human disc nucleus pulposus cells and the relationship between CC and BMP-7. *Euro Spine J* 2017;26:240–7. <https://doi.org/10.1007/s00586-016-4439-y>.
- [11] Zaniboni E, Bagne L, Camargo T, do Amaral MEC, Felonato M, de Andrade TAM, dos Santos GMT, Caetano GF, Esquisatto MAM, Santamaria Jr M, Mendonça FAS. Do electrical current and laser therapies improve bone remodeling during an orthodontic treatment with corticotomy? *Clin Oral Investig* 2019;23:4083–97. <https://doi.org/10.1007/s00784-019-02845-9>.
- [12] Wu M, Wu S, Chen W, Li YP. The roles and regulatory mechanisms of TGF- β and BMP signaling in bone and cartilage development, homeostasis and disease. *Cell Res* 2024;34. <https://doi.org/10.1038/s41422-023-00918-9>.
- [13] Glatt V, Evans CH, Stoddart MJ. Regenerative rehabilitation: the role of mechanotransduction in orthopaedic regenerative medicine. *J Orthopaedic Res* 2019;37:1263–9. <https://doi.org/10.1002/jor.24205>.
- [14] Janssens K, ten Dijke P, Janssens S, Van Hul W. Transforming growth factor- β 1 to the bone. *Endocr Rev* 2005;26:743–74. <https://doi.org/10.1210/er.2004-0001>.
- [15] Gillman CE, Jayasuriya AC. FDA-approved bone grafts and bone graft substitute devices in bone regeneration. *Mater Sci Eng* 2021;130:112466. <https://doi.org/10.1016/j.msec.2021.112466>.
- [16] Dixon DT, Gomillion CT. 3D-Printed conductive polymeric scaffolds with direct current electrical stimulation for enhanced bone regeneration. *J Biomed Mater Res B Appl Biomater* 2023;111. <https://doi.org/10.1002/jbm.b.35239>.
- [17] Zhang X, Wang T, Zhang Z, Liu H, Li L, Wang A, Ouyang J, Xie T, Zhang L, Xue J, Tao W. Electrical stimulation system based on electroactive biomaterials for bone tissue engineering. *Mater Today* 2023;68. <https://doi.org/10.1016/j.matod.2023.06.011>.
- [18] deVet T, Jhirad A, Pravato L, Wohl GR. Bone bioelectricity and bone-cell response to electrical stimulation: a review. *Crit Rev Biomed Eng* 2021;49:1–19. <https://doi.org/10.1615/CritRevBiomedEng.2021035327>.
- [19] Chaudhari SD, Sharma KK, Marchetto JJ, Hydren JR, Burton BM, Moreno AP. Modulating OPG and TGF- β 1 mRNA expression via bioelectrical stimulation. *Bone Rep* 2021;15:101141. <https://doi.org/10.1016/j.bonr.2021.101141>.
- [20] Puttini I, Poli P, Maiorana C, Vasconcelos I, Schmidt L, Colombo L, Hadad H, Santos G, Carvalho P, Souza F. Evaluation of osteoconduction of biphasic calcium phosphate ceramic in the calvaria of rats: microscopic and histometric analysis. *J Funct Biomater* 2019;10:7. <https://doi.org/10.3390/jfb10010007>.
- [21] Leppik L, Zhihua H, Mobini S, Thottakkattumana Parameswaran V, Eischen-Loges M, Slavici A, Helbing J, Pindur L, Oliveira KMC, Bhavsar MB, Hudak L, Henrich D, Barker JH. Combining electrical stimulation and tissue engineering to treat large bone defects in a rat model. *Sci Rep* 2018;8:6307. <https://doi.org/10.1038/s41598-018-24892-0>.
- [22] Zhang W, Wang N, Yang M, Sun T, Zhang J, Zhao Y, Huo N, Li Z. Periosteum and development of the tissue-engineered periosteum for guided bone regeneration. *J Orthop Translat* 2022;33:41–54. <https://doi.org/10.1016/j.jot.2022.01.002>.
- [23] Chen Y, Wang J, Zhu XD, Tang ZR, Yang X, Tan YF, Fan YJ, Zhang XD. Enhanced effect of β -tricalcium phosphate phase on neovascularization of porous calcium phosphate ceramics: *in vitro* and *in vivo* evidence. *Acta Biomater* 2015;11:435–48. <https://doi.org/10.1016/j.actbio.2014.09.028>.
- [24] Nguyen KQT, Olesen P, Ledet T, Rasmussen LM. Bone morphogenetic proteins regulate osteoprotegerin and its ligands in human vascular smooth muscle cells. *Endocrine* 2007;32:52–8. <https://doi.org/10.1007/s12020-007-9007-0>.
- [25] Rahman MS, Akhtar N, Jamil HM, Banik RS, Asaduzzaman SM. TGF- β /BMP signaling and other molecular events: regulation of osteoblastogenesis and bone formation. *Bone Res* 2015;3:15005. <https://doi.org/10.1038/boneres.2015.5>.